

## Fractal Properties of Robust Strange Nonchaotic Attractors

Brian R. Hunt\* and Edward Ott†

University of Maryland, College Park, Maryland 20742-2431

(Received 22 January 2001; published 29 November 2001)

For a simple class of quasiperiodically forced dynamical systems, we present a rigorous result supporting the idea that the attractors for this class of systems, although nonchaotic, are strange in the sense that their box-counting dimension is two while their information dimension is one. Furthermore, this result is stable to changes of the system, suggesting that the basic features leading to it may be present in typical quasiperiodically forced systems.

DOI: 10.1103/PhysRevLett.87.254101

PACS numbers: 05.45.Df, 05.45.Ac, 05.45.Pq

The external forcing of a nonlinear dynamical system is of general interest in many situations. For example, temporally periodic forcing can lead to the phenomenon of frequency locking and may also induce chaotic evolution of otherwise nonchaotic systems. Temporally random forcing causing escape of a particle from a potential well is a classic model in chemical kinetics. Between temporally periodic and random forcing is the case of quasiperiodic forcing, the case of interest in this paper.

A key aspect of quasiperiodic forcing of a nonlinear dynamical system is that it appears to make possible a fundamentally different kind of motion not seen in periodically forced systems. In particular, typical quasiperiodically forced nonlinear systems appear capable of supporting attractors that are nonchaotic (i.e., possess no positive Lyapunov exponents), yet at the same time are geometrically strange in that they exhibit nontrivial fractal properties. The possible existence of such *strange nonchaotic attractors* in quasiperiodically forced systems was originally pointed out in Ref. [1], and there has since been much analysis and numerical experimentation [2,3] as well as laboratory experimental realizations (e.g., Ref. [4]). Recently there have also been rigorous results on the mathematical properties these strange nonchaotic attractors must have if they exist [5].

In spite of these previous works, a very basic question still remains: Can it be shown analytically that strange nonchaotic attractors exist in a typical quasiperiodically forced system, and are they robust? Here, by robust we mean that arbitrarily small changes of the system cannot cause the strange nonchaotic attractor to no longer exist. The previous literature [1–4] certainly suggests that the answer to the question is yes, but can we really be sure? References [1,2] prove the existence of strange nonchaotic attractors for a particular class of quasiperiodically forced systems, but this class is such that an arbitrarily small change of the system can put it out of the class. The numerical and experimental evidence for strange nonchaotic attractors in typical quasiperiodically forced systems [3,4] is very strong, but perhaps the attractors observed are nonstrange with very fine scale structure (rather than the *infinitesimally* fine scale structure of a truly strange attrac-

tor). Also there might be the worry that the numerical evidence is somehow an artifact of computational errors. In this paper we address these concerns by examining the behavior of a simple class of quasiperiodically forced systems for which rigorous results are accessible. Furthermore, we demonstrate the nature of the strangeness of these attractors.

In general, a two-frequency quasiperiodically forced system of ordinary differential equations can be written in the form  $dx/dt = \mathbf{F}(\mathbf{x}, \xi, \theta)$ , where  $\mathbf{F}$  is  $2\pi$  periodic in the angles  $\xi$  and  $\theta$ , which are given by  $\xi = \omega_\xi t + \xi_0$ ,  $\theta = \omega_\theta t + \theta_0$ , and  $\omega_\xi$  and  $\omega_\theta$  are incommensurate. Sampling the state of the system at the times  $t_n$  given by  $\xi = 2n\pi$ , the ordinary differential equation system yields a mapping of the form  $\theta_{n+1} = (\theta_n + \omega) \bmod 2\pi$ ,  $\mathbf{x}_{n+1} = \tilde{\mathbf{F}}(\mathbf{x}_n, \theta_n)$ , where  $\mathbf{x}_n = \mathbf{x}(t_n)$ ,  $\omega = 2\pi\omega_\theta/\omega_\xi$ , and we assume  $\omega_\theta/\omega_\xi$  is irrational [for our numerical work  $\omega_\theta/\omega_\xi = (\sqrt{5} - 1)/2$ , the golden mean]. In what follows we examine the simplest case where the state variable  $\mathbf{x}$  is one dimensional. Specifically, we take  $\mathbf{x}$  to be an angle  $\varphi$  and we consider the map of the two-dimensional  $\theta$ - $\varphi$  torus,

$$\theta_{n+1} = (\theta_n + \omega) \bmod 2\pi, \quad (1a)$$

$$\varphi_{n+1} = [\theta_n + \varphi_n + \eta P(\theta_n, \varphi_n)] \bmod 2\pi, \quad (1b)$$

where  $P(\theta, \varphi)$  is continuous, differentiable, and  $2\pi$  periodic in both of its arguments. For  $\eta$  small enough,  $|\eta| < \eta_c$ , this map is invertible [solvable for  $(\theta_n, \varphi_n)$  given  $(\theta_{n+1}, \varphi_{n+1})$ ]. For  $P(\theta, \varphi) = \sin\varphi$ , which we use in our numerical work, the system is invertible if  $|\eta| < 1$ .

A crucial property of the map (1) is illustrated in Fig. 1. Figure 1 shows the  $\theta$ - $\varphi$  toroidal surface with a curve  $C$  drawn on it. Note that  $C$  circles around the torus in the  $\theta$  direction, but does not wrap around the torus in the  $\varphi$  direction. After one iterate of (1), the curve  $C$  is mapped to a curve  $C'$  that wraps once around the torus in the  $\varphi$  direction. Applying the map to  $C'$  produces a curve with two wraps around the torus in the  $\varphi$  direction, and so on. This behavior comes about due to the term  $\theta_n$  on the right-hand side of (1b), because  $\theta + \varphi + \eta P(\theta, \varphi)$  increases by  $2\pi$  as  $\theta$  increases by  $2\pi$ .

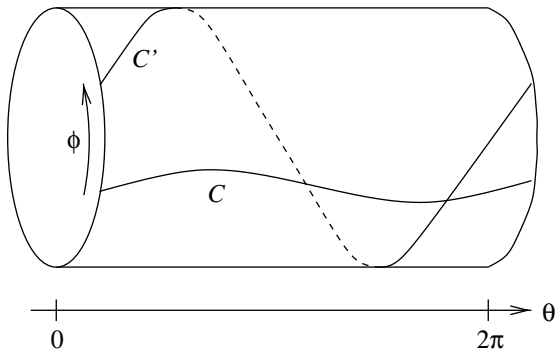


FIG. 1. Torus unwrapped in the  $\theta$  direction ( $\theta = 0$  and  $\theta = 2\pi$  are identified with each other). The map (1) takes the curve  $C$  to the curve  $C'$ .

A trajectory of the map (1) has two Lyapunov exponents  $h_\theta$  and  $h_\varphi$ , where  $h_\theta = 0$  is associated with (1a) and  $h_\varphi$  is associated with (1b). The latter exponent is given by the formula,

$$h_\varphi = \int \ln[1 + \eta P_\varphi(\theta, \varphi)] d\mu, \quad (2)$$

where  $P_\varphi = \partial P / \partial \varphi$ , and  $\mu$  denotes the measure generated by the orbit from a given initial point  $(\theta_0, \varphi_0)$ .

If  $h_\varphi > 0$  for a particular trajectory, then, since  $h_\theta = 0$ , the map exponentially expands areas near the trajectory in the limit  $n \rightarrow \infty$ . Since the  $\theta$ - $\varphi$  torus has finite area (namely,  $4\pi^2$ ), if the map is invertible, then there cannot be a set of initial points with positive area that have exponential area expansion along their trajectories. Therefore the set of initial points for which  $h_\varphi > 0$  has zero area (Lebesgue measure zero), and the map thus does not have a chaotic attractor.

Our main results are as follows: For  $|\eta| < \eta_c$ , (i) the map (1) has a single attractor; (ii) for typical  $P(\theta, \varphi)$ , the attractor has a Lyapunov exponent  $h_\varphi$  that is negative for  $\eta \neq 0$ ; (iii) the attractor has information dimension one for  $\eta \neq 0$ ; (iv) the attractor is the entire  $\theta$ - $\varphi$  torus and, hence, has box-counting dimension two [6]; (v) these results are stable to perturbations of the system [7].

For (ii) we do not have a rigorous proof; rather, we have an approximate analytical formula for  $h_\varphi$  for small  $\eta$ , and we show that it agrees well with numerical results. If we accept this, then (iii) follows [8]. Our proof of (i) and (iv) and their stability to perturbations (v) is mathematically rigorous.

Results (iii) and (iv) quantify the strangeness of the attractor. In particular, by (iii), orbits spend most of their time on a curvelike set; yet, by (iv), if one waits long enough each orbit eventually visits any neighborhood on the  $\theta$ - $\varphi$  torus. One can get a sense of this result from the numerical orbit shown in Fig. 2, in which a trajectory of length  $10^4$  appears to be concentrated along one-dimensional strands [Fig. 2(a)], but for the same parameters a trajectory of length  $10^5$  fills much more of the  $\theta$ - $\varphi$  torus [Fig. 2(b)].

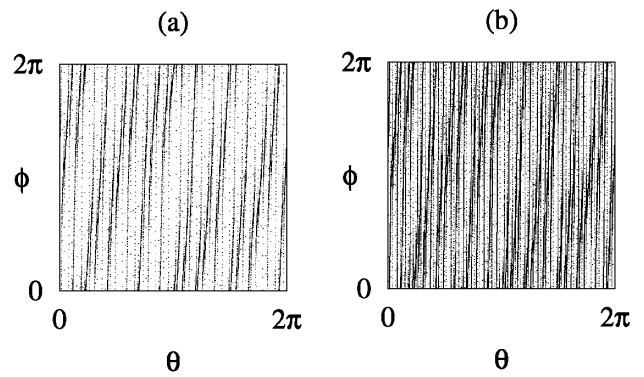


FIG. 2. Trajectory of the map (1) with  $\omega = \pi(\sqrt{5} - 1)$ ,  $\eta = 0.3$ , and  $P(\theta, \varphi) = \sin \varphi$ . In each case  $\theta_0 = \varphi_0 = 0$  and  $10^4$  points of the trajectory are computed before plotting; in (a) the next  $10^4$  points are plotted, while (b) shows  $10^5$  points.

A numerical experiment to determine the information and box-counting dimensions both illustrates points (iii) and (iv), and indicates why it is hard to obtain convincing conclusions for the dimension values based only on numerics. We show in Fig. 3(a) a plot of  $\log_2 N(\varepsilon)$  versus  $\log_2(1/\varepsilon)$ , and in Fig. 3(b) a plot of  $\sum p_i \log_2(1/p_i)$  versus  $\log_2(1/\varepsilon)$ . Here  $N(\varepsilon)$  is the number of  $\varepsilon \times \varepsilon$  boxes (in  $\theta$ - $\varphi$  space) needed to cover the points from an orbit of length  $T$ , and  $p_i$  is the fraction of those orbit points in the  $i$ th  $\varepsilon \times \varepsilon$  box. According to claim (iv) [claim (iii)], in the limit  $T \rightarrow \infty$ , the points in Fig. 3(a) [Fig. 3(b)] should follow a straight line of slope two [one] for small  $\varepsilon$ , corresponding to a box-counting [information] dimension of two [one]. As is commonly found, the box-counting dimension computation converges rather slowly with increasing orbit length  $T$ . Thus, we show plots in Fig. 3 for several different  $T$ . As can be seen in Fig. 3(a), the  $\varepsilon$  range consistent with a slope of two (the straight line in the figure) steadily increases toward smaller  $\varepsilon$  [larger  $\log(1/\varepsilon)$ ] as  $T$  increases. This is in contrast with Fig. 3(b), which appears to reach a form independent of  $T$  that is consistent with a small  $\varepsilon$  slope of one. While the convergence

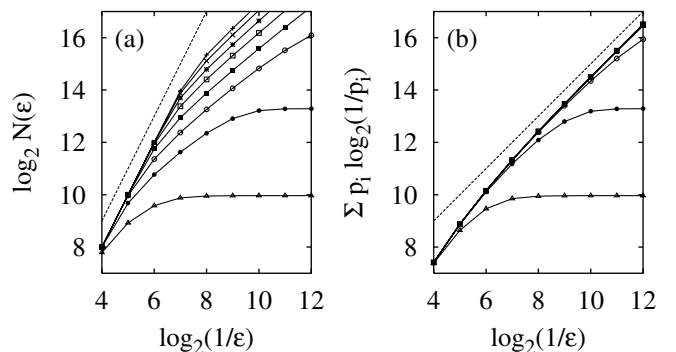


FIG. 3. Dimension computations for (1) with  $\eta = 0.5$ ,  $\omega = \pi(\sqrt{5} - 1)$ , and  $P(\theta, \varphi) = \sin \varphi$ . In (a) the dashed line has slope two, while in (b) it has slope one. In each graph, the curves from lowest to highest represent  $T = 10^3, 10^4, \dots, 10^{10}$ ; in (b) the final five curves are virtually identical.

in Figs. 3(a) and 3(b) is consistent with box-counting and information dimensions of two and one, the slowness of the convergence also indicates that a purely numerical determination of the dimension values is suspect. Next we give a heuristic argument for (ii), from which (iii) follows, and a proof for (iv).

To see that  $h_\varphi < 0$  for small nonzero  $\eta$ , consider first the case  $\eta = 0$ , for which (1b) becomes  $\varphi_{n+1} = (\theta_n + \varphi_n) \bmod 2\pi$ . If we initialize a uniform distribution of orbit points in the  $\theta$ - $\varphi$  torus then, on one application of the  $\eta = 0$  map, the distribution remains uniform. Furthermore, this uniform distribution is generated by the orbit from any initial condition. To verify this, we note the explicit form of an  $\eta = 0$  orbit,  $\theta_n = (\theta_0 + n\omega) \bmod 2\pi$ ,  $\varphi_n = [\varphi_0 + n\theta_0 + \frac{1}{2}(n^2 - n)\omega] \bmod 2\pi$ , which is shown to generate a uniform density in Ref. [9]. We can obtain an approximation to  $h_\varphi$  for nonzero but small  $\eta$  by expanding  $\ln(1 + \eta P_\varphi)$  in (2) to order  $\eta^2$  and assuming that, to this order, the deviation of the measure  $\mu$  from uniformity is not significant [ $d\mu \approx d\theta d\varphi / (2\pi)^2$ ]. Using  $\ln(1 + \eta P_\varphi) = \eta P_\varphi - (1/2)\eta^2 P_\varphi^2 + O(\eta^3)$ , this gives

$$h_\varphi = -\frac{1}{2}\eta^2 \langle P_\varphi^2 \rangle + o(\eta^2), \quad (3)$$

which is negative for small enough  $\eta \neq 0$ . Here  $\langle P_\varphi^2 \rangle$  denotes the  $\theta$ - $\varphi$  average of  $P_\varphi^2$ , and the order  $\eta$  term is absent by virtue of  $\int_0^{2\pi} P_\varphi d\varphi = 0$ . Figure 4 shows a plot of  $h_\varphi$  versus  $\eta$  for  $P(\theta, \varphi) = \sin\varphi$ . Remarkably, Eq. (3) (the straight line) describes the numerical data to better than 8% even for  $\eta$  as large as 0.5.

To establish results (i) and (iv), that the attractor of the map (1) is the whole  $\theta$ - $\varphi$  torus, we prove that the map is *topologically transitive*: For every pair of open disks  $A$  and  $B$ , there is a trajectory that starts in  $A$  and passes through  $B$ . This property is known to imply that a dense set of initial conditions yield trajectories that are dense in

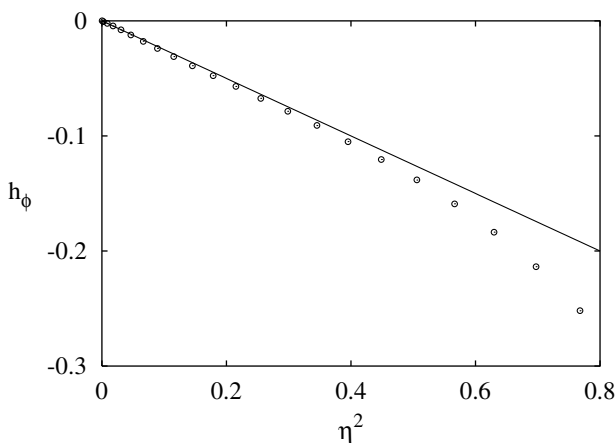


FIG. 4. Lyapunov exponent  $h_\varphi$  versus  $\eta^2$ . For each  $\eta$ , the data plotted as open circles were computed from  $10^9$  iterations of the map (1) with  $\omega = \pi(\sqrt{5} - 1)$  and  $P(\theta, \varphi) = \sin\varphi$ .

the torus [10]. In particular, any attractor, having an open basin of attraction, must contain a dense orbit, and, hence, must be the entire torus.

We will show that, for every pair of horizontal line segments  $L_a = [\theta_a, \theta_a + \delta] \times \{\varphi_a\}$  and  $L_b = [\theta_b, \theta_b + \delta] \times \{\varphi_b\}$ , there is a (finite) trajectory that begins on the first line segment and ends on the second. (Choosing  $L_a$  to lie in  $A$  and  $L_b$  to lie in  $B$ , this implies topological transitivity.) Our strategy is to iterate  $L_a$  forward until the union of these iterates includes every value of  $\theta$  at least once; the number of iterates needed is finite and depends only on  $\delta$ . By throwing away pieces of some of these iterates, we form the graph  $\varphi = g_a(\theta)$  of a piecewise continuous function  $g_a$ . Similarly, we form a graph  $\varphi = g_b(\theta)$  from pieces of backward iterates of  $L_b$ . Finally, we show that some forward iterate of the graph  $\varphi = g_a(\theta)$  must intersect the graph  $\varphi = g_b(\theta)$ .

The following is a formal definition of  $g_a$ . For each  $\theta$ , let  $k(\theta)$  be the smallest non-negative integer for which  $\{[\theta - k(\theta)\omega] \bmod 2\pi\} \in [\theta_a, \theta_a + \delta]$ . That is,  $k(\theta)$  is the minimum number of backward iterates of Eq. (1a) from  $\theta$  required to land in the interval  $[\theta_a, \theta_a + \delta]$ . Let  $g_a(\theta)$  be the  $\varphi$  coordinate of the  $k(\theta)$ th iterate of  $[\theta - k(\theta)\omega, \varphi_a]$ , and let  $K$  be the maximum value of  $k(\theta)$ . Then the graph  $\varphi = g_a(\theta)$  has a finite number  $d \leq K + 1$  discontinuities, and each continuous piece of this graph is a forward iterate of some piece of  $L_a$ .

Now form the curve  $G_a$  by taking the graph of  $g_a$  and adding vertical line segments at each point, where  $g_a$  is discontinuous so as to make  $G_a$  a continuous curve. Notice that, for each  $n$ , the  $n$ th iterate of  $G_a$  is also a continuous curve that consists of the graph of a function with  $d$  discontinuities together with  $d$  vertical line segments.

Define  $g_b$  and  $G_b$  similarly to  $g_a$  and  $G_a$ , but in terms of the backward (not forward) iterates of the line segment  $L_b$ . Notice that, because  $L_a$  and  $L_b$  have the same length  $\delta$ , the function  $g_b$  (similar to  $g_a$ ) has  $d$  discontinuities.

Our goal is to show that, for  $n$  sufficiently large, the  $n$ th iterate of  $G_a$  intersects  $G_b$  for at least  $2d + 1$  different values of  $\theta$ . Then since there are at most  $2d$  values of  $\theta$  at which one of these two curves has a vertical segment, there is at least one intersection between the  $n$ th iterate of the graph of  $g_a$  and the graph of  $g_b$ , whence some point on  $L_a$  maps to some point on  $L_b$  in at most  $2K + n$  iterates.

Given a continuous curve  $C$  that, similar to  $G_a$  and  $G_b$ , is the graph of a function together with a finite number of vertical line segments at discontinuities of the function, observe that its image under the map (1) is a curve of the same type (in particular, since the map is one-to-one, the lengths of the vertical segments remain between 0 and  $2\pi$ ). Furthermore, because of the  $\theta_n$  term in the equation for  $\varphi_{n+1}$ , the image of  $C$  “wraps around” the torus in the  $\varphi$  direction one more time than  $C$  does as one goes around the torus one time in the  $\theta$  direction (cf. Fig. 1).

To formulate what we mean by “wrapping around,” define the winding number of  $C$  as follows. As  $\theta$  increases

from 0 to 1, count the number of times  $C$  crosses the circle  $\varphi = 0$  in the upward and downward directions. The difference between the number of upward and downward crossings is the winding number of  $C$ .

Now if two curves  $C_1$  and  $C_2$  have different winding numbers  $w_1$  and  $w_2$ , then  $C_1$  and  $C_2$  must intersect at least  $|w_1 - w_2|$  times. Because of the periodicity of  $P(\theta, \varphi)$ , the winding number of a curve must increase by one each time the map (1) is applied. Thus, for  $n$  sufficiently large, the winding number of the  $n$ th iterate of  $G_a$  differs from the winding number of  $G_b$  by at least  $2d + 1$ . Hence, the  $n$ th iterate of  $G_a$  intersects  $G_b$  for at least  $2d + 1$  different values of  $\theta$ . This establishes claims (i) and (iv).

Notice that the argument above does not depend on the specific form of  $P(\theta, \varphi)$ , only that it is continuous and periodic and that  $\eta$  is sufficiently small ( $|\eta| < \eta_c$ ) that the map (1) is one-to-one. This independence of the results from the specific form of  $P(\theta, \varphi)$  implies that the results are stable to system changes [our claim (v)] that preserve a quasiperiodic driving component (1a).

We now show that stability to perturbations applies in addition if the system is higher dimensional. In particular, we discuss the case of a three-dimensional system with an attracting invariant torus, and allow perturbations of the toroidal surface. Consider the following map on  $\mathbf{R}^3$ :

$$\theta_{n+1} = (\theta_n + \omega) \bmod 2\pi, \quad (4a)$$

$$\varphi_{n+1} = [\theta_n + \varphi_n + \eta \bar{P}(\theta_n, \varphi_n, r_n)] \bmod 2\pi, \quad (4b)$$

$$r_{n+1} = \lambda r_n + \rho Q(\theta_n, \varphi_n, r_n). \quad (4c)$$

Here  $\theta$  and  $\varphi$  are coordinates on a torus embedded in  $\mathbf{R}^3$ , as in Fig. 1, and  $r$  is a coordinate in the direction perpendicular to the torus, with  $r = 0$  representing the torus itself. The parameters  $\omega$  and  $\eta$ , and the dependence of  $\bar{P}$  on  $\theta$  and  $\varphi$ , have the same properties as for map (1), and  $Q$  is continuously differentiable. When  $\lambda$  and  $\rho$  are small, Eqs. (4) map a neighborhood of the torus  $r = 0$  into itself, and when  $\rho = 0$  the torus  $r = 0$  is invariant and attracting. It then follows from classical results on the perturbation of invariant manifolds [11] that, for  $\lambda$  and  $\rho$  sufficiently small, the map (4) has a smooth attracting invariant manifold  $r = f(\theta, \varphi)$  near the torus  $r = 0$ . On this attractor, the map (4) reduces to a map of the form (1), with  $P(\theta, \varphi) = \bar{P}[\theta, \varphi, f(\theta, \varphi)]$ . Thus statements (i)–(v) above apply also to the attractor of the three-dimensional map (4).

In conclusion, our rigorous analysis of the map (1) provides firm evidence for the existence of strange nonchaotic attractors as a generic phenomenon of quasiperiodically forced systems.

We thank J. Stark for encouragement and discussion. This research was supported by the Office of Naval Re-

search (Division of Physics), the National Science Foundation (Divisions of Mathematical and Physical Sciences), and the W. M. Keck Foundation.

\*Institute for Physical Science and Technology, and Department of Mathematics.

†Institute for Plasma Research, Department of Physics, and Department of Electrical and Computer Engineering.

- [1] C. Grebogi, E. Ott, S. Pelikan, and J. A. Yorke, *Physica* (Amsterdam) **13D**, 261 (1984).
- [2] G. Keller, *Fundam. Math.* **151**, 139 (1996).
- [3] Some examples of numerical and analytical studies are the following: A. Bondeson, E. Ott, and T. M. Antonsen, *Phys. Rev. Lett.* **55**, 2103 (1985); F. J. Romeiras *et al.*, *Physica* (Amsterdam) **26D**, 277 (1987); J. F. Heagy and S. M. Hammel, *Physica* (Amsterdam) **70D**, 140 (1994); A. S. Pikovsky and U. Feudel, *Chaos* **5**, 253 (1995); A. Witt, U. Feudel, and A. S. Pikovsky, *Physica* (Amsterdam) **109D**, 180 (1977); A. Prasad, V. Mehra, and R. Ramaswamy, *Phys. Rev. Lett.* **79**, 4127 (1997); *Phys. Rev. E* **57**, 1576 (1998); T. Nishikawa and K. Kaneko, *Phys. Rev. E* **54**, 6114 (1996); T. Yalcinkaya and Y. C. Lai, *Phys. Rev. Lett.* **77**, 5039 (1996); M. Ding, C. Grebogi, and E. Ott, *Phys. Rev. A* **39**, 2593 (1989); A. Prasad *et al.*, *Phys. Rev. Lett.* **83**, 4530 (1999).
- [4] W. L. Ditto *et al.*, *Phys. Rev. Lett.* **65**, 533 (1990); T. Zhou, F. Moss, and A. Bulsara, *Phys. Rev. A* **45**, 5397 (1992).
- [5] J. Stark, *Physica* (Amsterdam) **109D**, 163 (1997); R. Sturman and J. Stark, *Nonlinearity* **13**, 113 (2000).
- [6] A previous study presented numerical evidence and heuristic arguments for the attractor of the two-dimensional map example of Ref. [1] having box-counting dimension two and information dimension one [M. Ding, C. Grebogi, and E. Ott, *Phys. Lett. A* **137**, 167 (1989)].
- [7] In the current paper we are concerned with robust strange nonchaotic attractors. The apparent strange nonchaotic attractors for the experiments of Ref. [4] seem to be of this type. For other systems, arbitrarily small parameter change may make the attractor nonstrange, but strange nonchaotic attractors may still be typical in the sense that they occupy a nonzero volume of the parameter space. Systems where strange nonchaotic attractors seem to have this character are discussed by Bondeson *et al.*, Romeiras *et al.*, and Ding *et al.* [3].
- [8] The information dimension cannot be less than one due to the quasiperiodic  $\theta$  dynamics, and cannot be more than one due to the fact that Lyapunov dimension is an upper bound on information dimension [F. Ledrappier, *Commun. Math. Phys.* **81**, 229 (1981)].
- [9] H. Furstenberg, *Am. J. Math.* **83**, 573 (1961).
- [10] See, for example, A. Katok and B. Hasselblatt, *Introduction to the Modern Theory of Dynamical Systems* (Cambridge University Press, Cambridge, England, 1995).
- [11] R. Sacker, *J. Math. Mech.* **18**, 705 (1969); N. Fenichel, *Indiana Univ. Math. J.* **21**, 193 (1971).